NeuroImage: Clinical 32 (2021) 102850

Contents lists available at ScienceDirect

NeuroImage: Clinical

journal homepage: www.elsevier.com/locate/ynicl

Neuroimaging correlates of gait abnormalities in progressive supranuclear palsy

Irene Sintini [a,*], Kenton Kaufman [b], Hugo Botha [c], Peter R. Martin [d], Stacy R. Loushin [b], Matthew L. Senjem [a,e], Robert I. Reid [e], Christopher G. Schwarz [a], Clifford R. Jack Jr [a], Val J. Lowe [a], Keith A. Josephs [c], Jennifer L. Whitwell [a], Farwa Ali [c]

[a] Department of Radiology, Mayo Clinic, Rochester, MN 55905, USA
[b] Department of Orthopedic Surgery, Mayo Clinic, Rochester, MN 55905, USA
[c] Department of Neurology, Mayo Clinic, Rochester, MN 55905, USA
[d] Department of Health Science Research, Mayo Clinic, Rochester, MN 55905, USA
[e] Department of Information Technology, Mayo Clinic, Rochester MN 55905, USA

ARTICLE INFO

Keywords:
Progressive supranuclear palsy
Diffusion tensor imaging
Gait
Balance
MRI
PET

ABSTRACT

Progressive supranuclear palsy is a neurodegenerative disorder characterized primarily by tau inclusions and neurodegeneration in the midbrain, basal ganglia, thalamus, premotor and frontal cortex. Neurodegenerative change in progressive supranuclear palsy has been assessed using MRI. Degeneration of white matter tracts is evident with diffusion tensor imaging and PET methods have been used to assess brain metabolism or presence of tau protein deposits. Patients with progressive supranuclear palsy present with a variety of clinical syndromes; however early onset of gait impairments and postural instability are common features. In this study we assessed the relationship between multimodal imaging biomarkers (i.e., MRI atrophy, white matter tracts degeneration, flortaucipir-PET uptake) and laboratory-based measures of gait and balance abnormalities in a cohort of nineteen patients with progressive supranuclear palsy, using univariate and multivariate statistical analyses. The PSP rating scale and its gait midline sub-score were strongly correlated to gait abnormalities but not to postural imbalance. Principal component analysis on gait variables identified velocity, stride length, gait stability ratio, length of gait phases and dynamic stability as the main contributors to the first component, which was associated with diffusion tensor imaging measures in the posterior thalamic radiation, external capsule, superior cerebellar peduncle, superior fronto-occipital fasciculus, body and splenium of the corpus callosum and sagittal stratum, with MRI volumes in frontal and precentral regions and with flortaucipir-PET uptake in the precentral gyrus. The main contributor to the second principal component was cadence, which was higher in patients presenting more abnormalities on mean diffusivity: this unexpected finding might be related to compensatory gait strategies adopted in progressive supranuclear palsy. Postural imbalance was the main contributor to the third principal component, which was related to flortaucipir-PET uptake in the left paracentral lobule and supplementary motor area and white matter disruption in the superior cerebellar peduncle, putamen, pontine crossing tract and corticospinal tract. A partial least square model identified flortaucipir-PET uptake in midbrain, basal ganglia and

Abbreviations: ACR, anterior corona radiata; ALIC, anterior limb of internal capsule; BCC, body of the corpus callosum; BoS, base of support; CGC, cingulate gyrus; CGH, cingulum (hippocampus); COP, center of pressure; CP, cerebral peduncle; CTS, corticospinal tract; CV, coefficient of variation; DTI, diffusion tensor imaging; EC, external capsule; FA, fractional anisotropy; FDG, fluorodeoxyglucose; GCC, genu of the corpus callosum; ICP, inferior cerebellar peduncle; MCP, middle cerebellar peduncle; MD, mean diffusivity; MDS - UPDRS, Movement Disorder Society - sponsored revision of the Unified Parkinson's Disease Rating Scale; ML, medial lemniscus; PC, principal component; PCA, principal component analysis; PCR, posterior corona radiata; PCT, pontine crossing tract; PLIC, posterior limb of internal capsule; PLS, partial least square; Postural imbalance EC, postural imbalance with eyes closed; Postural imbalance EO, postural imbalance with eyes open; PSP, progressive supranuclear palsy; PSP-RS, progressive supranuclear palsy – Richardson's syndrome; PSP-P, progressive supranuclear palsy – parkinsonism; PSP-PGF, progressive supranuclear palsy – progressive freezing of gait; PSP – SL, progressive supranuclear palsy – speech and language; PSP-CBS, progressive supranuclear palsy – corticobasal syndrome; PTR, posterior thalamic radiation; RLIC, retrolenticular part of internal capsule; RMSE, root mean square error; ROI, region of interest; SCC, splenium of the corpus callosum; SCP, superior cerebellar peduncle; SCR, superior corona radiata; SLF, superior longitudinal fasciculus; SFO, superior fronto-occipital fasciculus; SS, sagittal stratum; SUVR, standard uptake value ratios; xCOM, extrapolated center of mass.

* Corresponding author at: Mayo Clinic, 200 1st St. SW, Rochester, MN 55905, USA.
E-mail address: sintini.irene@mayo.edu (I. Sintini).

https://doi.org/10.1016/j.nicl.2021.102850
Received 19 July 2021; Received in revised form 24 September 2021; Accepted 2 October 2021
Available online 12 October 2021

thalamus as the main correlate of speed and dynamic component of gait in progressive supranuclear palsy. Although causality cannot be established in this analysis, our study sheds light on neurodegeneration of brain regions and white matter tracts that underlies gait and balance impairment in progressive supranuclear palsy.

1. Introduction

Progressive supranuclear palsy (PSP) is a neurodegenerative proteinopathy characterized by neuronal loss and neuronal and glial four repeat (4R) tau inclusions in cardinal regions of the brain (Dickson et al. 2010). On neuroimaging, patients with PSP show reduced grey and white matter volume in the midbrain, thalamus, basal ganglia, middle cingulate and premotor regions of the frontal lobe on structural MRI (Price et al. 2004, Josephs et al. 2013) and white matter degeneration of the dentatorubrothalamic tract, including the superior cerebellar peduncle, body of the corpus callosum, posterior thalamic radiations and association tracts such as the superior longitudinal fasciculus, on diffusion tensor imaging (DTI) (Canu et al. 2011, Whitwell et al. 2011a, Whitwell et al. 2011b). *In vivo* tau pathology in PSP patients can be imaged with PET ligands such as [^{18}F] flortaucipir. Although the pathological specificity of flortaucipir remains uncertain, several studies reported *in vivo* flortaucipir-PET uptake in PSP patients in key regions, such as the dentate nucleus of the cerebellum, midbrain, globus pallidus and thalamus (Passamonti et al. 2017, Schonhaut et al. 2017, Smith et al. 2017, Whitwell et al. 2017, Cope et al. 2018, Sintini et al. 2019), with the signal increasing over time (Whitwell et al. 2019). Flortaucipir-PET uptake has been associated with neurodegenerative changes in PSP in recent literature (Sintini et al. 2019, Malpetti et al. 2020, Nicastro et al. 2020).

Clinically, PSP most often presents with PSP-Richardson's syndrome (PSP-RS), which is characterized by postural instability, akinetic rigidity and vertical supranuclear gaze palsy. However, PSP is also associated with several other clinical phenotypes, such as parkinsonism (PSP-P), progressive freezing of gait (PSP-PGF), speech and language (PSP-SL), or corticobasal syndrome (PSP-CBS) (Hoglinger et al. 2017). Early onset of gait impairment, postural instability, and resulting falls, develop in most patients, regardless of phenotype, and are the primary cause of morbidity and mortality (Bluett et al. 2017). Three-dimensional motion analysis revealed that PSP patients have significantly decreased gait speed, cadence and stride length, increased step width, impaired gait initiation and abnormal dynamic postural stability compared to healthy controls (Amano et al. 2015, Ali et al. 2021). PSP patients also have more severe gait impairment than patients with Parkinson's disease (Egerton et al. 2012, Kammermeier et al. 2018a, Kammermeier et al. 2018b, Raccagni et al. 2018, De Vos et al. 2020), from early disease stage (Amboni et al. 2021).

Understanding whether and how neuroimaging markers are related to gait and balance impairment in PSP is a crucial step towards understanding their pathophysiology, development of patient-centered outcomes and ultimately effective therapies and interventions. Few studies have investigated the relationships between neuroimaging and motion variables in PSP. One study identified hypometabolism in the thalamus as a correlate of balance deficits and falls, with a compensatory role of the precentral gyrus (Zwergal et al. 2011), in sixteen PSP participants. Another study found that, during walking, functional activation of the prefrontal cortex, subthalamic nucleus and thalamus was reduced in twelve patients with PSP, while it was increased in the precentral gyrus and cerebellar vermis (Zwergal et al. 2013), compared to healthy controls. A more recent study found associations between gait initiation impairment and hypometabolism in areas of the supraspinal locomotor network, including the caudate, supplementary motor area, cingulate cortex, thalamus, and midbrain (Palmisano et al. 2020).

In this study, we assess relationships between multimodal neuroimaging (i.e., structural MRI, DTI, flortaucipir-PET and fluorodeoxyglucose (FDG)-PET) and laboratory-based measures of gait and balance impairment in a cohort of nineteen PSP patients. We hypothesize that different measures of gait and balance impairment will be related to neurodegenerative change in distinct sets of brain regions known to be affected by this disease.

2. Materials and methods

2.1. Participants

Nineteen participants meeting the 2017 Movement Disorder Society diagnostic criteria for PSP (Hoglinger et al. 2017) were recruited from the Department of Neurology, Mayo Clinic, Rochester, MN, by the Neurodegenerative Research Group (NRG) between July 2019 and November 2020. All participants met the 2017 Movement Disorder Society clinical criteria for PSP, including the clinical phenotypes of PSP-RS, PSP-P, PSP-SL, and PSP-CBS; none met criteria for PSP-PGF. All participants were able to ambulate independently with minimal assistance and were excluded if they were immobile due to advanced disease stage or an alternative explanation for gait impairment, such as significant orthopedic issues. All participants underwent a detailed neurological evaluation, which included two standardized scales: the Movement Disorder Society - sponsored revision of the Unified Parkinson's Disease Rating Scale part III (MDS-UPDRS III) and the PSP rating scale (sub-scales: history, mentation, bulbar, ocular motor, limb motor, gait midline). Demographic and clinical features of the participants are reported in Table 1. This study was approved by the Mayo Clinic Internal Review Board and informed written consent was obtained from each participant prior to data collection.

2.2. Neuroimaging

The 3 T head MRI protocol included: a magnetization prepared rapid gradient echo (MPRAGE) sequence (TR/TE/TI = 2300/3.14/945 ms, flip angle 9°, 0.8 mm isotropic resolution, field of view 256x240 mm); a diffusion weighted spin echo single shot Echo Planar Imaging (EPI) sequence, with 2.0 mm isotropic voxels, 13b = 0, 6b = 500, 48b = 1000, and 60b = 2000 s/mm^2 volumes in each scan, with the diffusion gradients in each shell evenly spread using an electrostatic repulsion scheme (Caruyer et al. 2013), modified to distribute them over whole

Table 1
Demographic and clinical features.

PSP phenotype		13 PSP-RS
		3 PSP-P
		1 PSP-CBS
		2 PSP-SL
PSP rating scale	Total score	39 ± 10
	History	9 ± 3
	Mentation	3 ± 2
	Bulbar	3 ± 2
	Ocular motor	7 ± 3
	Limb motor	5 ± 3
	Gait midline	12 ± 4
MDS-UPDRS III		49 ± 17
Disease duration (year)		4.7 ± 2.6
Age at exam (year)		71 ± 7
Height (cm)		169 ± 10
Weight (Kg)		80 ± 21
Sex		11 M
		8F

Numbers are reported as mean and standard deviation.

spheres instead of hemispheres. All MRI scans were acquired on one of two Prisma scanners (Siemens Healthcare, Erlangen, Germany). PET scans were acquired using a PET/CT scanner (GE Healthcare, Milwaukee, Wisconsin or Siemens Healthcare, Erlangen, Germany) operating in 3D mode. For flortaucipir-PET, an intravenous bolus injection of approximately 370 MBq (range 333–407 MBq) of flortaucipir was administered, followed by a 20-minute PET acquisition performed 80 min after injection. Flortaucipir scans consisted of four 5-minute dynamic frames following a low dose CT transmission scan. Nine of the nineteen participants (one PSP-P, eight PSP-RS) also underwent FDG-PET within two months of MRI. Participants were injected with [^{18}F] FDG of approximately 459 MBq (range 367–576 MBq) and, after a 30-minute uptake period, an 8-minute FDG-PET scan was acquired consisting of four 2-minute dynamic frames following a low dose CT transmission scan. Standard corrections were applied.

Each PET image was rigidly registered to its corresponding MPRAGE using SPM12 (Wellcome Trust Centre for Neuroimaging, London, UK). Using ANTs, the Mayo Clinic Adult Lifespan Template (MCALT) (https://www.nitrc.org/projects/mcalt/) atlases were propagated to the native MPRAGE space and used to calculate regional PET values in grey and white matter regions-of-interest (ROIs). Tissue probabilities were determined for each MPRAGE using Unified Segmentation in SPM12, with MCALT tissue priors and settings. The cortical ROIs included frontal and sensorimotor regions that have been shown to be affected on neuroimaging in PSP (supplementary motor area, precentral, postcentral, paracentral, mid-cingulate, superior and medial frontal) and macro-ROIs covering medial and lateral parietal regions that are less affected in the disease. The cerebellum, cerebellar crus, vermis and pons were also included. Subcortical grey matter structures included the pallidum, putamen, caudate, and thalamus. The cortical and subcortical ROIs were defined using MCALT. The midbrain, superior cerebellar peduncle, and dentate nucleus of the cerebellum were manually drawn on the MCALT atlas, as previously described (Whitwell et al. 2019). The subthalamic nucleus, red nucleus, and substantia nigra ROIs were defined using the Deep Brain Stimulation Intrinsic atlas (Ewert et al. 2018). The median PET value in each ROI was divided by median uptake in cerebellar crus grey matter for flortaucipir and in the pons for FDG to create standard uptake value ratios (SUVR). PET images were not partial volume corrected to keep MRI and PET measurements relatively independent from each other for the multimodal analyses. Tissue volume (grey and white matter combined) was calculated in the same set of ROIs. We used tissue volume because in the deep brain grey matter structures, which are key regions in PSP, the grey versus white matter segmentation has poor contrast in T1-weighted MRI, so we combined the segmented grey and white matter probabilities and relied on the atlas normalization to determine the region boundaries instead. We used tissue volume in cortical regions because PSP is a disease that affects both grey and white matter on the cortex. The DTI images (fractional anisotropy (FA) and mean diffusivity (MD)) were processed as described previously (Schwarz et al. 2014), and the median DTI scalar values (FA, MD) were measured within specific white matter tracts in the Johns Hopkins University "Eve" single-subject atlas (Oishi et al. 2009), including corticospinal tract (CST), inferior cerebellar peduncle (ICP), medial lemniscus (ML), superior cerebellar peduncle (SCP), cerebral peduncle (CP), anterior and posterior limb of internal capsule (ALIC, PLIC), posterior thalamic radiation (PTR), anterior, superior and posterior corona radiata (ACR, SCR, PCR), cingulate gyrus (CGC), cingulum (hippocampus) (CGH), superior longitudinal fasciculus (SLF), superior fronto-occipital fasciculus (SFO), sagittal stratum (SS), external capsule (EC), pontine crossing tract (PCT), middle cerebellar peduncle (MCP), genu, body and splenium of the corpus callosum (GCC, BCC, SCC), retrolenticular part of internal capsule (RLIC). Since PSP is commonly a symmetrical syndrome, we merged left and right ROIs and tracts to reduce the number of variables in statistical analyses. Structural MRI, DTI and PET images of each subject were subsequently spatially normalized to the MCALT template and blurred with an 8 mm (DTI) or 6 mm (MRI, PET) full width at half maximum kernel for voxel-wise analyses. While the voxel approach is more data-driven but has less power, the ROI approach is more hypothesis-driven, imposing a set of regions and an atlas beforehand and therefore making a priori assumptions about the data.

2.3. Motion analysis

A summary of the motion analysis protocol is reported below. More details on gait and balance measurements in a subset of the current PSP patients have been previously reported (Ali et al. 2021).

2.3.1. Standing postural balance

The participants stood for 30 s with each foot on a force plate (Optima HPS, AMTI, Watertown, MA, 600 Hz). Participants were tested looking directly ahead with 1) eyes open (EO) and 2) eyes closed (EC). Three participants were not able to perform this test. For both test conditions, the metrics that were subsequently calculated to quantify static balance were the position of the net center of pressure (COP) under the foot, its root mean square error (RMSE), and the extrapolated center of mass (xCOM) (Hof 2008).

2.3.2. Gait

Forty-one reflective markers were placed on each participant with respect to bony landmarks, using a modified Helen-Hayes marker set to create local coordinate systems for each segment. For safety, the participants wore a harness which was attached to a track in the ceiling such that if a fall occurred, the patient would never encounter the ground. The participants walked barefoot on a 10-meter walkway at their self-selected speed. A minimum of three trials were performed by each participant. A ten camera motion capture system (Raptor-12, Motion Analysis Corporation, Santa Rosa, CA, 120 Hz) was used to collect three-dimensional marker trajectories from the reflective markers. Ground reaction forces were collected using five force plates (Optima HPS, AMTI, Watertown, MA, 600 Hz) embedded in the walkway. To quantify efficiency of locomotion, the global spatiotemporal parameters of stride length, cadence, velocity, step width, gait stability ratio, length of gait phases as percent of gait cycle including total support and initial double limb support, were calculated from the marker data using the center of the heel as the reference point on the foot (Sutherland et al. 1988, Heitmann et al. 1989).These parameters were averaged across three gait trials. Gait phases were averaged between the left and right leg to reduce the number of variables, since no specific asymmetry was identified. The coefficient of variation was calculated on the stride length to estimate inter-step variability. Additionally, the average distance between the xCOM and the base of support (BoS) (Rosenblatt and Grabiner 2010) at heel strike, normalized with respect to the height of the participant, was calculated to quantify dynamic stability; this quantity was also averaged between the left and right leg. Dynamic stability was available for eighteen out of nineteen patients. Table 2 provides a brief description of the motion laboratory variables used in this study.

2.4. Statistical analysis

Spearman's rank correlations were performed between motion laboratory variables and clinical scores as well as ROI-level neuroimaging quantities. Total intracranial volume was regressed out from the MRI regional volumes before performing all the statistical analyses. Age was not included as a covariate because it correlated with PSP-RS ($R = 0.51$, $p = 0.026$) and correcting for age would have therefore erased part of the effect of the disease, which was not acceptable given the small sample size. Spearman's rank correlations were favored over Pearson's because they are less sensitive to outliers, which can be especially problematic when the number of data points is limited. Statistical significance was set at $p < 0.05$. These correlations were repeated on the sub-group of thirteen patients with PSP-RS clinical presentation and reported as

Table 2
Description of motion laboratory variables.

Motion laboratory variable	Description
Stride length	Length of a stride (cm), calculated as the distance between the proximal end position of the foot at ipsilateral heel strike to the proximal end of the next ipsilateral heel strike. It is a global spatiotemporal measure.
Cadence	Steps per minute. It is a global spatiotemporal measure.
Velocity	Stride length multiplied by cadence and divided by two (cm/sec). It is a global spatiotemporal measure.
Step width	Width of a step (cm), calculated as the medial–lateral distance between the proximal end position of the foot at ipsilateral heel strike to the proximal end position of the foot at the next contralateral heel strike. It is a global spatiotemporal measure.
Gait stability ratio	Cadence divided by velocity. A higher gait stability ratio indicates that a larger portion of the gait cycle is spend in double limb support, decreasing the dynamic component of walking and increasing stability (Cromwell and Newton 2004). It is a global spatiotemporal measure.
Total support	Amount of time the foot spends on the ground. It is a global spatiotemporal measure.
Initial double support	Amount of time both feet are on the ground after initial contact. It is a global spatiotemporal measure.
Postural imbalance	Root mean square error of the center of pressure when the participant stands on force plates for 30 s with eyes open or eyes closed.
Dynamic stability	Average distance between the extrapolated center of mass and the base of support during gait, normalized with respect to the height of the participant.

supplemental. Correlations between gait variables and FDG-PET uptake are also reported as supplemental; in these correlations, the midbrain regions were excluded because their signal is close to the pons, which was the reference region. Correlations between motion laboratory variables and FDG-PET and flortaucipir-PET SUVR with partial volume correction are reported as supplemental. Spearman's correlations between clinical scores (i.e., PSP rating scale and sub-scales, MDS-UPDRS III) and imaging quantities are also reported as supplemental. Two multivariate approaches were subsequently applied. First, a principal component analysis (PCA) was performed on gait and balance metrics to reduce the number of variables, identifying the main patterns of variation in the data and diminishing the problem of multiple comparisons. Then, SPM12 was used to perform one-sample *t*-tests that assessed the effect of the principal components on each imaging modality. Results were assessed at $p < 0.001$. Secondly, a partial least squares (PLS) regression model was used to find latent structures that correlate regional neuroimaging and gait matrices. PLS identifies translations of both datasets that are maximally correlated with each other, explaining how patterns of variability in regional neuroimaging metrics are related to patterns of variability in gait metrics, and can also be thought of as fitting multiple univariate models simultaneously. Specifically, we used an approach like the multimodal PLS previously described (Chen et al. 2009) to associate the combined information from *z*-scored regional imaging quantities (the independent matrix) to global spatiotemporal gait metrics (the dependent matrix). The PLS algorithm incorporates information from both the independent and the dependent variables simultaneously to define the PLS loadings and scores on both the independent and dependent matrices. The following gait parameters were included: velocity, cadence, stride length, step width, gait stability ratio, total support phase and initial double limb support. The PLS model did not include static and dynamic stability quantities to maximize the number of participants included in this analysis, since these two quantities were not available for three of the participants. The statistical analyses were performed in Matlab 2018a (The Mathworks, Inc., Natick, MA, USA) and R version 3.6.0 (http://www.r-project.org/).

3. Results

3.1. Univariate analyses

Spearman's correlations between clinical scores and gait variables are shown in Table 3. Compared to healthy controls, velocity, cadence, stride length and dynamic stability are typically lower in PSP patients, while step width, gait stability ratio, total support, initial double support, postural imbalance, and stride length coefficient of variation are typically higher. PSP rating scale and MDS-UPDRS III scores strongly correlated to velocity, stride length, gait stability ratio and dynamic stability. The gait midline sub-scale score of the PSP rating scale strongly correlated to velocity, dynamic stability, and stride length coefficient of variation. In contrast, all the other PSP rating sub-scale scores were not significantly associated with any gait variable (not shown in Table 3), except for ocular motor and history. The history sub-score was unexpectedly negatively associated with step width.

Correlations between neuroimaging ROI-based quantities and gait lab variables are shown in Fig. 1. Typically, DTI-FA and MRI volumes are reduced in PSP relative to healthy controls, while DTI-MD and flortaucipir SUVR are increased.

Velocity: Velocity was negatively correlated to DTI-MD in the cerebellar peduncle (Fig. 1B) and positively correlated to volume in the supplementary motor area, superior frontal, and lateral parietal cortex (Fig. 1C). These associations were in the expected direction: velocity was higher in participants with higher volume and lower median diffusivity. Velocity was positively correlated to subcortical flortaucipir-PET uptake (subthalamic nucleus, pallidum, caudate, red nucleus) (Fig. 1D). These associations were not in the expected direction, as one would expect higher flortaucipir-PET uptake, suggestive of neurodegeneration, to be related to lower velocity. Within the PSP-RS sub-group, there was no association between velocity and subcortical flortaucipir-PET uptake (Supplemental Fig. 2D).

Cadence: Cadence was positively associated with DTI-MD in various tracts, especially the sagittal stratum and the cingulum (hippocampus) (Fig. 1B). Higher cadence was related to more abnormalities on imaging, which was unexpected. In the PSP-RS sub-group, higher cadence was strongly correlated to higher DTI-MD in the cingulum (hippocampus) (Supplemental Fig. 2B).

Stride length: Stride length was strongly associated with DTI-MD in the body and splenium of the corpus callosum (Fig. 1B) and with volume in the precentral, superior, and medial frontal, and parietal cortex (Fig. 1C). A strong positive association to lateral parietal volume was also present in the PSP-RS sub-group (Supplemental Fig. 2C). Stride length was also associated with DTI-FA in the anterior corona radiata, sagittal stratum and splenium of the corpus callosum (Fig. 1A), and with flortaucipir-PET uptake in the precentral (Fig. 1D). Shorter stride length was associated with more abnormalities on imaging. As with velocity, stride length was also unexpectedly positively correlated with higher flortaucipir-PET uptake in the subthalamic nucleus (Fig. 1D). Within the PSP-RS sub-group, there was no association between stride length and subcortical flortaucipir-PET uptake (Supplemental Fig. 2D).

Step width: Step width was strongly related to DTI-MD in the superior cerebellar peduncle (Fig. 1B) and flortaucipir-PET uptake in the dentate nucleus, cerebellum, and pons (Fig. 1D). A strong positive association to DTI-MD in the superior cerebellar peduncle and flortaucipir-PET uptake in the cerebellum was also present in the PSP-RS sub-group (Supplemental Fig. 2B, 2D). Step width was also related to DTI-FA if the corticospinal tract, cingulate gyrus, external capsule, middle cerebellar peduncle, and body of the corpus callosum (Fig. 1A) and superior frontal volume (Fig. 1C). Within the PSP-RS sub-group, there were several strong associations between step width and DTI-FA, particularly in the anterior limb of the internal capsule, cingulum, external capsule, and body of the corpus callosum (Supplemental Fig. 2A). As hypothesized, higher step width was related to more imaging abnormalities in the identified regions. However, step width was also unexpectedly

Table 3
Spearman's correlation coefficients between motion laboratory variables and clinical scores.

	Direction of change in PSP	PSP rating scale	PSP rating scale - history	PSP rating scale – ocular motor	PSP rating scale – gait midline	MDS-UPDRS III
Velocity	PSP < Controls	−0.68*	−0.51	–	−0.72*	−0.7*
Cadence	PSP < Controls	−0.49	–	−0.48	−0.57	–
Stride Length	PSP < Controls	−0.58*	−0.47	–	−0.53	−0.71*
Step Width	PSP > Controls	–	−0.52	–	–	–
Gait Stability Ratio	PSP > Controls	0.58*	0.48	–	0.54	0.71*
Total Support	PSP > Controls	0.46	–	–	–	0.5
Initial Double Support	PSP > Controls	0.48	–	–	–	0.52
Postural Imbalance EO	PSP > Controls	–	–	–	–	–
Postural Imbalance EC	PSP > Controls	–	–	–	–	–
Dynamic Stability	PSP < Controls	−0.61*	–	–	−0.63*	−0.64*
Stride Length CV	PSP > Controls	0.51	–	–	0.66*	–

Only the sub-scales of the PSP rating scale that showed significant correlations are reported.
Only correlations with $p < 0.05$ are reported. Correlations with $p < 0.01$ are marked with an asterisk.
The column 'Direction of change in PSP' illustrates in which direction gait quantities are typically altered in PSP relative to normal controls.

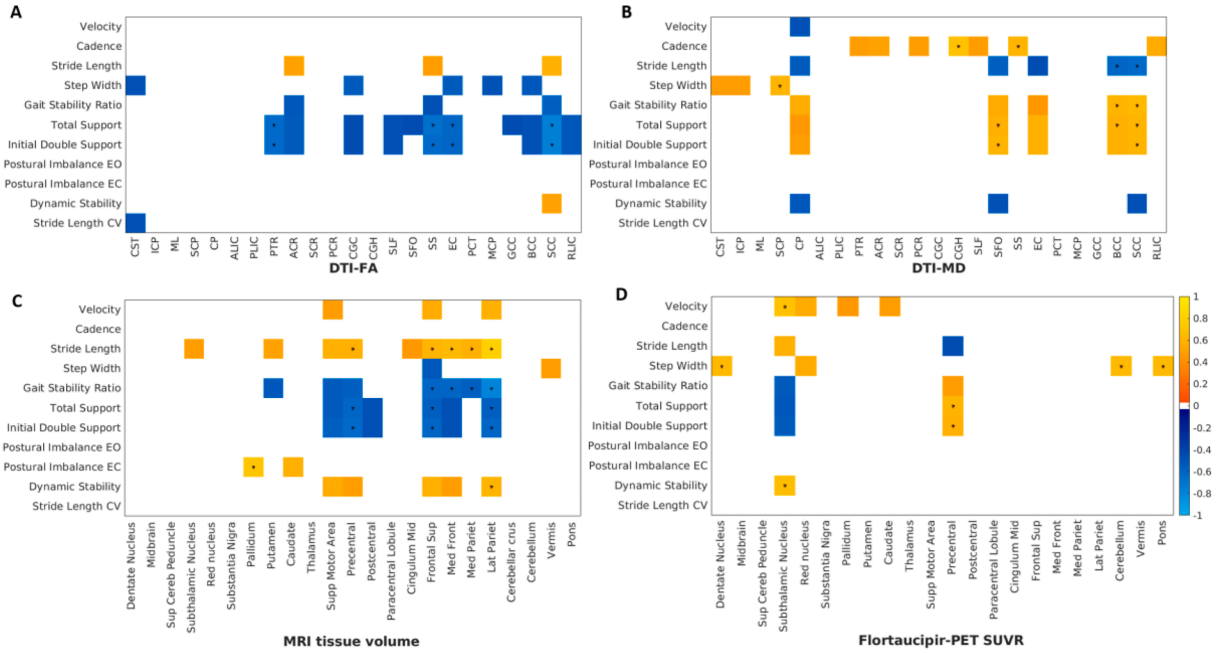

Fig. 1. Correlations between gait, balance, and neuroimaging quantities. Spearman's correlations between motion quantities and ROI-based imaging quantities from DTI-FA (A), DTI-MD (B), MRI volume (C) and flortaucipir-PET SUVR (D). Only correlations with $p < 0.05$ are reported. Correlations with $p < 0.01$ are marked with an asterisk. The color bar on the right refers to the Spearman's correlation coefficient values.

positively correlated with the volume of the vermis (Fig. 1C) and with glucose metabolism in the subthalamic nucleus (Supplemental Fig. 1).

Gait stability ratio: Gait stability ratio exhibited associations with imaging analogous to stride length, but in opposite direction, as expected (Fig. 1).

Total support: Total support time was higher (i.e., more impaired gait) in patients with lower DTI-FA in many tracts, particularly the posterior thalamic radiation, sagittal stratum, external capsule and splenium of the corpus callosum (Fig. 1A) and higher DTI-MD in the superior fronto-occipital fasciculus, body and splenium of the corpus callosum (Fig. 1B). In the PSP-RS sub-group, the strongest association was with DTI-FA in the posterior corona radiata (Supplemental Fig. 2A). Patients with greater total support time also had lower volumes, particularly in the precentral, superior frontal and lateral parietal regions (Fig. 1C), higher flortaucipir-PET uptake in the precentral (Fig. 1D), and lower glucose metabolism in the lateral parietal cortex, cerebellum and cerebellar crus (Supplemental Fig. 2). All these relationships were in the expected direction. Total support time was unexpectedly positively correlated to higher flortaucipir-PET uptake in the subthalamic nucleus (Fig. 1D), but not in the PSP-RS sub-group (Supplemental Fig. 2D).

Initial double support: Initial double support was mostly analogous to total support in its associations with imaging. Additionally, it demonstrated a negative correlation to metabolism in the thalamus (Supplemental Fig. 1).

Postural imbalance: Greater postural imbalance with eyes open correlated to reduced metabolism in the cerebellar crus and lateral parietal cortex and greater postural imbalance with eyes closed correlated to reduced metabolism in the dentate nucleus (Supplemental Fig. 1). Greater postural imbalance with eyes closed was unexpectedly correlated to higher volume of the pallidum and caudate (Fig. 1C). In the PSP-RS sub-group, more associations were present between greater postural imbalance with eyes open and increased imaging abnormalities, like lower DTI-FA (Supplemental Fig. 2A) and higher DTI-MD (Supplemental

Fig. 2B) in the splenium of the corpus callosum, lower precentral, postcentral, lateral parietal and cerebellum volume (Supplemental Fig. 2C), higher flortaucipir-PET uptake in the supplementary motor area, precentral, paracentral lobule, middle cingulate and superior frontal (Supplemental Fig. 2D).

Dynamic stability: Lower dynamic stability strongly correlated with lower volume in the lateral parietal cortex (Fig. 1C). This association was present in the PSP-RS sub-group too (Supplemental Fig. 2C). It also correlated with lower volume in the supplementary motor area, precentral, superior and medial frontal (Fig. 1 C), lower DTI-FA in the splenium of the corpus callosum (Fig. 1A), and higher DTI-MD in the cerebellar peduncle, superior fronto-occipital fasciculus and splenium of the corpus callosum (Fig. 1B). Consistently with what was found for other gait variables, higher dynamic stability was also unexpectedly associated with higher flortaucipir-PET uptake in the subthalamic nucleus (Fig. 1D), but not in the PSP-RS sub-group (Supplemental Fig. 2D).

Stride length variation: Higher stride length variation correlated to lower DTI-FA in the corticospinal tract (Fig. 1A) and lower metabolism in the cerebellar crus (Supplemental Fig. 1).

Partial volume correction applied on PET data did not substantially change the results, but it did reveal superior frontal flortaucipir SUVR (Supplemental Fig. 3A) and vermis FDG SUVR (Supplemental Fig. 3B) as important correlates of gait variables.

Relationships between clinical scores (i.e., PSP rating scale scores and sub-scores and MDS-UPDRS III) and neuroimaging regional quantities are shown Supplemental Fig. 4. Clinical scores showed positive correlations with DTI measures of white matter tract degeneration in several regions, particularly the cerebellar peduncle (Supplemental Fig. 4A, 4B). PSP rating scale limb motor sub-score and MDS-UPDRS III were strongly correlated with volume in frontal, supplementary motor, and parietal regions (Supplemental Fig. 4C). The unexpected negative correlation between the MDS-UPDRS III score and flortaucipir-PET uptake in the subthalamic nucleus is consistent with the associations found with gait variables (Supplemental Fig. 4D).

3.2. Multivariate analyses

The first three principal components, which accounted for more than 98% of the variability in the data, are represented in Fig. 2 with their correlations to the gait and balance variables ($p < 0.01$). PCA identified velocity, stride length, gait stability ratio, length of gait phases and dynamic stability as the main contributors to the first principal component (PC1, 71% of variability), which represented a measure of overall severity in gait impairment. Patients with lower PC1 scores had more abnormal gait, with reduced stride length, velocity and dynamic stability, higher gait stability ratio, and longer total support and initial double support phases. PC1 was strongly correlated with both age ($R = -0.63$, $p = 0.007$) and PSP rating scale score ($R = -0.66$, $p = 0.005$), but not with disease duration. Cadence and postural imbalance were the main contributors to the second (PC2, 24% of variability) and third (PC3, 3% of variability) components, respectively. Participants with higher PC2 scores had higher cadence, while participants with higher PC3 scores had greater postural imbalance. Both PC2 and PC3 were not correlated to either age or PSP rating scale score. The first three PC scores along with phenotype, PSP rating score and gait and balance variables are reported in Supplemental Table 1. Although velocity was derived from the product of stride length and cadence, the ways in which these three quantities vary were independent, as identified by PCA. Variation in stride length was the main driver of variation in velocity, while variation in cadence was more limited and therefore its effect on velocity less pronounced (Supplemental Fig. 5A). Velocity and stride length were strongly correlated, while the same was not true for velocity and cadence (Supplemental Fig. 5B). These trends were specific for this PSP population and may represent the evolving gait disorder or compensatory gait changes in PSP.

3.2.1. DTI-FA and PC scores

Patients with lower PC1 scores (i.e., worse gait performance) had lower DTI-FA in the corpus callosum, cingulum, superior longitudinal fasciculus, anterior limb of the internal capsule, sagittal stratum, superior frontal (Fig. 3). Associations between DTI-FA and PC2 and PC3 were limited to few voxels: patients with higher scores on PC2 (i.e., higher cadence) had lower DTI-FA in few voxels in the right superior parietal and middle temporal regions, which was unexpected, and patients with higher PC3 scores (i.e., more postural instability) had lower DTI-FA in the right putamen (Fig. 3).

3.2.2. DTI-MD and PC scores

Patients with lower PC1 scores had higher DTI-MD in the cerebellar peduncle, superior longitudinal fasciculus, posterior limb of the internal capsule, thalamus, cingulum, splenium of corpus callosum (Fig. 3). Patients with higher PC2 had higher DTI-MD in a few voxels in the left middle occipital region, which was unexpected and consistent with the ROI-based findings (Fig. 1B). Patients with higher PC3 had higher DTI-MD in the superior cerebellar peduncle, putamen, pontine crossing tract and corticospinal tract (Fig. 3).

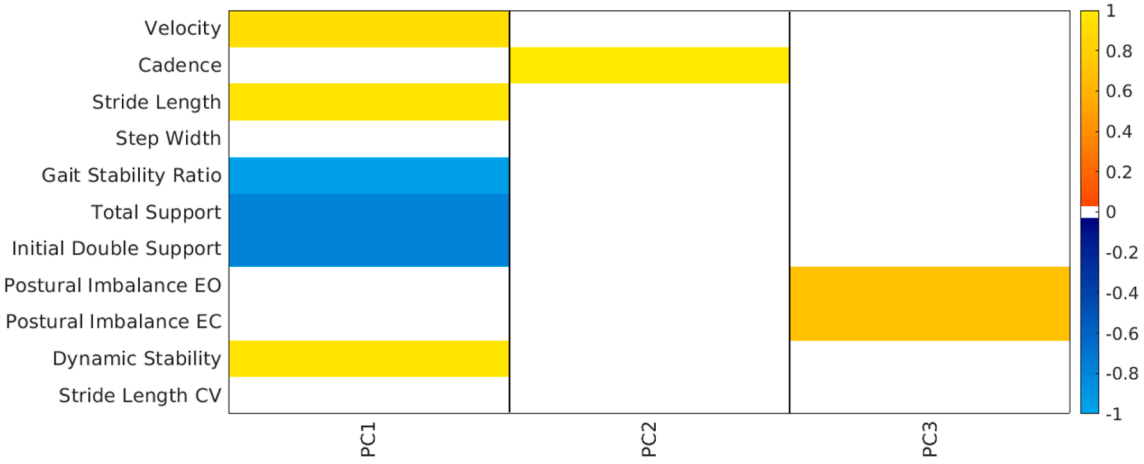

Fig. 2. Principal component analysis on gait and balance quantities. Spearman's correlation coefficients ($p < 0.01$) between principal component scores from PCA performed on gait global spatiotemporal variables, postural imbalance and dynamic stability and the same quantities (e.g. PC1 is highly correlated with velocity, stride length and dynamic stability, therefore participants with higher PC1 scores have increased velocity, stride length and dynamic stability). PC1 explained 71% of the variability, PC2 24% and PC3 3%.

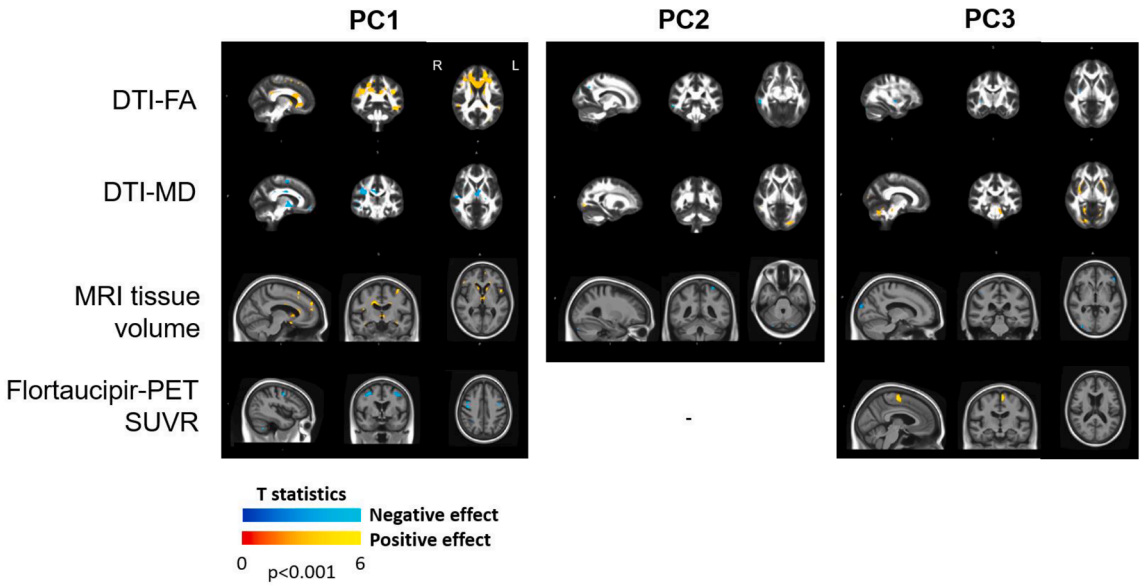

Fig. 3. Effect of principal component scores on neuroimaging. Effect of the first three principal component scores on DTI-FA, DTI-MD, MRI volume and flortaucipir-PET SUVR. Sixteen participants with complete motion laboratory data were included. Results are shown at $p < 0.001$.

3.2.3. *MRI volume and PC scores*

Patients with lower PC1 scores had smaller volumes in the frontal lobe, precentral and thalamus (Fig. 3). Patients with higher PC2 scores had smaller volumes in few voxels in the left superior parietal regions, which was a finding not in the expected direction. Patients with higher PC3 scores had smaller volumes in few voxels in the right occipital and left inferior frontal regions (Fig. 3).

3.2.4. *Flortaucipir-PET SUVR and PC scores*

Patients with lower PC1 scores had higher flortaucipir-PET uptake in bilateral precentral gyrus, whereas those with higher PC3 scores had higher uptake in left paracentral lobule and supplementary motor area (Fig. 3).

3.2.5. *Partial least squares regression*

The first three components of the PLS model captured a large percentage of the variation in velocity (78%), cadence (65%), stride length (75%), step width (60%), gait stability ratio (70%), total support (64%) and initial double support (61%) phases. The PLS components captured the variance in the data with a descending order of magnitude. The first PLS component captured a high percent of variation in stride length (46%), total support (43%) and initial double support (40%) phases (Fig. 4A). Patients with higher scores on the first PLS component had a higher stride length and shorter total support and initial double support phases (i.e., lesser gait impairment). On neuroimaging, higher loads on this component were mostly associated with less imaging abnormalities. The highest loadings for the first PLS component were found in: DTI-FA of the sagittal stratum, anterior corona radiata, posterior thalamic radiation, corpus callosum; DTI-MD of the corpus callosum, superior longitudinal fasciculus, retrolenticular part of internal capsule; MRI volumes and flortaucipir-PET uptake of the precentral, supplementary motor and superior frontal areas (Fig. 4A). MRI volumes of the middle cingulate, parietal cortex, paracentral lobule and postcentral were also identified in the first PLS component (Fig. 4A). The second PLS

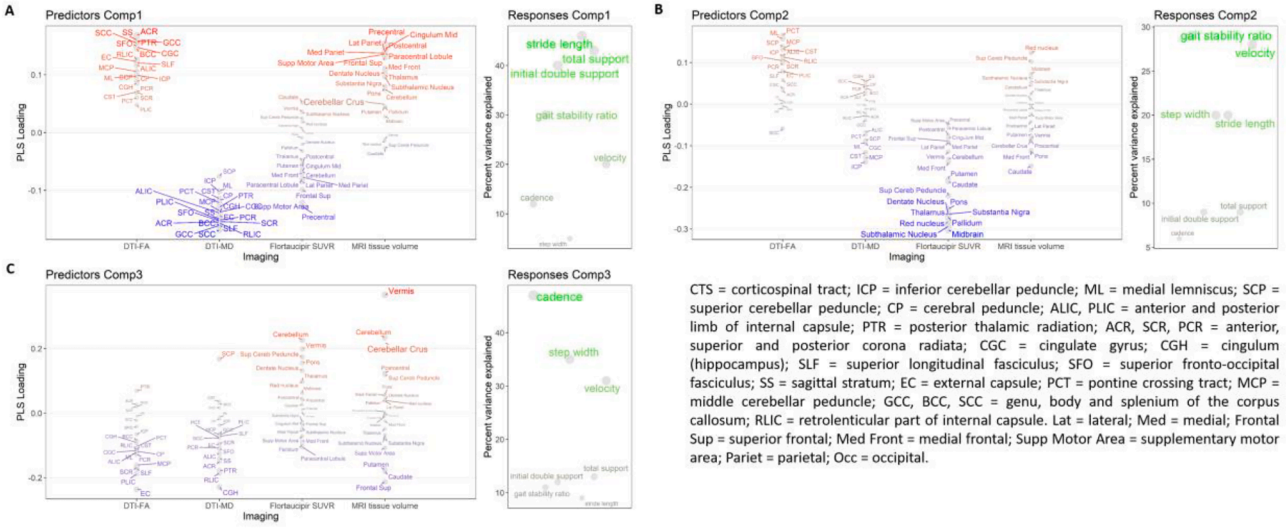

Fig. 4. PLS model on neuroimaging and gait global spatiotemporal parameters. PLS loadings for each imaging modality and explained variance of each gait variable for the first three PLS components. The PLS model was developed to predict the gait global spatiotemporal quantities from the imaging ROI-based data. Regions with higher loading magnitude contributed more strongly to the PLS components and are highlighted with more intense color and larger font size.

component captured variation mostly in velocity (28%) and gait stability ratio (29%). Patients with higher scores on the second PLS component had higher velocity and lower gait stability ratio (i.e., lesser gait impairment). On neuroimaging, the highest loadings were in flortaucipir-PET uptake of the midbrain, subthalamic nucleus, red nucleus, thalamus, pallidum, substantia nigra and pons (Fig. 4B). The third PLS component captured most of the variability in cadence (47%) and step width (35%). Patients with higher scores on the third PLS components had lower cadence and higher step width (i.e., greater gait impairment). The third PLS component was related to the imaging modalities in mixed directions: reduced DTI-FA (external capsule, posterior limb of the internal capsule), increased DTI-MD (superior cerebellar peduncle), increased flortaucipir-PET uptake (vermis, cerebellum, superior cerebellar peduncle), reduced MRI volumes (superior frontal, caudate, putamen), but also decreased DTI-MD in the cingulum (hippocampus), and larger volume in the vermis, cerebellum and cerebellar crus (Fig. 4C). Given the small size of the training set, the PLS model cannot be used as a predictive tool due to risk of overfitting, and its purpose was limited to describing the current data with a multivariate approach.

4. Discussion

We have presented a unique dataset comprising multimodal neuroimaging (DTI, MRI volumes and flortaucipir-PET) and laboratory-based measures of gait and balance in nineteen patients clinically diagnosed with PSP. FDG-PET was also investigated in nine of these patients. Global spatiotemporal gait parameters are worse in PSP relative to healthy controls (Egerton et al. 2012, Amano et al. 2015, Raccagni et al. 2018, Ali et al. 2021) and strongly correlated with PSP rating scale and MDS-UPDRS III scores. Employing univariate and multivariate analyses, we showed that gait and balance variables were associated with imaging abnormalities in regions commonly affected by PSP. On DTI, degenerative changes in white matter tracts that have been identified as among the most disrupted in PSP or related to the PSP system of neurodegeneration (Sintini et al. 2019, Nicastro et al. 2020, Whitwell et al. 2021), such as the posterior thalamic radiation, external capsule, superior cerebellar peduncle, superior fronto-occipital fasciculus, body and splenium of the corpus callosum and sagittal stratum, were related to reduced stride length, increased step width and longer total support and initial double support phases. On MRI, lower volume in regions that are part of the supraspinal locomotor network (Bohnen and Jahn 2013), such as superior and medial frontal, precentral, supplementary motor, lateral parietal, putamen and subthalamic nucleus, correlated with gait abnormalities. Prefrontal cortex is important for gait initiation (Jahn et al. 2008, Bohnen and Jahn 2013) and lower superior frontal volume strongly correlated to longer initial double support phase. Atrophy of the midbrain is a key radiographic feature of PSP but was not associated with motion abnormalities. This may be due to the temporal window during disease progression that was analyzed and lack of longitudinal data. An alternative explanation could be that, during undisturbed locomotion, brainstem regions can be bypassed using the direct pathway from the motor cortex to the spinal cord (Bohnen and Jahn 2013, Zwergal et al. 2013, Duysens and Nonnekes 2021). On the other hand, we did find that flortaucipir-PET uptake in the midbrain was the most important contributor to the second PLS component, which captured variability in velocity and gait stability ratio. We also found an association between larger step width and higher flortaucipir-PET uptake in the red nucleus, which points to the involvement of the midbrain in this gait variable.

Flortaucipir-PET uptake gave meaningful but also somewhat contradictory results. Specifically, increased flortaucipir SUVR in the precentral gyrus was associated with worse gait performances, while increased SUVR in the paracentral lobule and supplementary motor area was associated with greater postural instability. On the other hand, flortaucipir-PET uptake in the subthalamic nucleus unexpectedly correlated with less gait abnormalities. This finding was most likely driven by PSP-RS cases that tended to have higher uptake in the subthalamic nucleus compared to other variants, but also performed better in terms of velocity and dynamic stability. In fact, these associations were not present when the PSP-RS sub-group was analyzed separately. The same reasoning holds for flortaucipir-PET uptake in the red nucleus, pallidum and caudate, which positively correlated with velocity. This aspect will require further investigation with a larger and more phenotypically diverse cohort. However, it has already been demonstrated that PSP variants present different involvement of subcortical circuitry and PSP-RS patients have higher flortaucipir uptake in the midbrain, striatum and subthalamic nucleus (Whitwell et al., 2020). This controversial finding on flortaucipir-PET uptake was mirrored by an association between higher glucose metabolism in the subthalamic nucleus and larger step width, which marks a more impaired gait. Additionally, higher metabolism in the subthalamic nucleus was related to worse performance in all the other analyzed gait and balance variables, but these correlations did not reach statistical significance and therefore were not shown. In Parkinson's disease, abnormally high activity of the subthalamic nucleus inhibits movement through the basal ganglia-thalamocortical circuit and inhibition of the subthalamic nucleus through deep brain stimulation has been related to improved gait and posture clinical scores (Chen and Lemon 2004, Potter et al. 2004). A similar mechanism might be in place in PSP and, in that case, higher metabolism in the subthalamic nucleus would be a disease effect leading to the inhibition of normal movement. However, this explanation is only speculative and would need to be verified in a larger cohort of patients and with further analyses. In contrast, another study showed reduced activation of the subthalamic nucleus during walking in patients with PSP (Zwergal et al. 2013).

Postural imbalance did not extensively correlate with imaging abnormalities. This lack of associations could be explained by the limited amount of variation present in the postural imbalance data, which represented only 3% of the total variation, as identified by the third principal component. This principal component was higher (i.e., worse postural balance) in patients with greater DTI-MD in the superior cerebellar peduncle, putamen, pontine crossing tract and corticospinal tract, and higher flortaucipir-PET uptake in the left paracentral lobule and supplementary motor region. Additionally, lower metabolism in the dentate nucleus and cerebellar crus was associated to worse static balance, consistently with the literature (Tian et al. 2017). Patients with vascular disease that presented with PSP-like clinical features, such as early falls, exhibited lesions in the basal ganglia and thalamus, but not in the substantia nigra or subthalamic nucleus (Josephs et al. 2002). Thalamus hypometabolism has been associated with postural sway in PSP (Zwergal et al. 2011). In our cohort, hypometabolism in the red nucleus, pallidum, putamen, caudate and thalamus, but not in the subthalamic nucleus or substantia nigra, was related to postural imbalance with eyes open, but these correlations did not reach statistical significance and therefore were not reported. Hypometabolism in the supplementary motor area, cingulate cortex, thalamus, and midbrain has been implicated in poor postural stability at gait initiation (Palmisano et al. 2020). Analogously, we found that hypometabolism in the thalamus, lateral parietal cortex and cerebellar crus and lower volume in the supplementary motor area, precentral and postcentral regions were associated with impaired gait initiation expressed as longer initial double support phase. On the contrary, others have found that higher metabolism in the supplementary motor area and precentral gyrus correlated with impaired balance in PSP and interpreted this as a compensatory effort of the motor cortex (Zwergal et al. 2011). In our study, there were a few correlations between postural imbalance and MRI volumes that were unexpected: patients with greater volume in the pallidum and caudate also had worse static balance outcomes. It was found that functional activation of the vermis was increased during locomotor in PSP (Zwergal et al. 2013). Unlike for functional imaging, we cannot hypothesize a compensatory mechanism based on volume.

Instead, the correlation between larger pallidum and caudate volumes and worse balance and, similarly, the one between larger vermis volume and greater step width, might be marking effects like phenotype or age. These findings will need to be verified in a larger and more phenotypically diverse cohort. In fact, when the PSP-RS sub-group was analyzed separately, more associations between multimodal imaging abnormalities and postural imbalance were found, suggesting differences among PSP phenotypes. It is also important to realize that locomotion, postural control, and balance are complex phenomena and the imaging modalities analyzed here address only part of them. Synaptic loss could contribute to motor impairment in PSP in absence of atrophy (Holland et al. 2020) and abnormal otolith-mediated vestibular reflexes (Liao et al. 2008) and reduced thalamic cholinergic activity (Lindemann et al. 2010) have been proposed as possible causes of falls in PSP and Parkinson's disease.

The principal component analysis of motion laboratory variables separated variation in velocity, stride length, gait stability ratio, length of gait phases and dynamic stability (PC1) from variation in cadence (PC2) and in postural imbalance (PC3). Similarly, cadence and step width were captured mostly by the third PLS component, while velocity, stride length, gait stability ratio and duration of gait phases were captured by the first two. Patients with more severe neurodegenerative change on DTI-MD and, more mildly, on DTI-FA and MRI, had decreased velocity and stride length but increased cadence. Although PSP patients typically have reduced cadence compared to controls (Amano et al. 2015), a relative increase in cadence may represent a compensatory mechanism to maintain velocity, as they become more impaired and unable to increase their stride length. It has been shown that, during dual-task situations that involved a cognitive and a motor task, PSP patients who were frequent fallers changed their gait by decreasing stride length and increasing cadence significantly more than patients who were not frequent fallers (Lindemann et al. 2010). This is consistent with the notion that different brain mechanisms regulate stride length and cadence, as it has been reported for Parkinson's disease (Morris et al. 1996). Patients with advanced Parkinson's disease develop levodopa resistant gait and balance abnormalities similar to those seen in PSP, suggestive of common non-dopaminergic pathways underlying these abnormalities (Bohnen and Jahn 2013).

Results from the PLS model largely confirmed the findings from previous analyses. The first PLS component, which is the most important in terms of the amount of captured variance, identified DTI-FA in the sagittal stratum, anterior corona radiata, posterior thalamic radiation and corpus callosum, DTI-MD in the superior longitudinal fasciculus, corpus callosum and sagittal stratum, flortaucipir-PET uptake and MRI volumes in the precentral, supplementary motor area, and superior frontal cortex as the major contributors to the variance in total support and initial double support phases and stride length. MRI volume in the postcentral, paracentral, middle cingulate and lateral parietal cortex also contributed strongly to this component. In healthy older adults, higher grey matter mean diffusivity in the precuneus, anterior cingulate and middle cingulate cortex and white matter disruption in the body of the corpus callosum, association tracts and thalamic radiations have been associated to worse gait performances (Tian et al. 2016a, Tian et al. 2016b, Verlinden et al. 2016, Tian et al. 2017). Our findings reflect a more widespread change than what would be expected in normal aging. Velocity and gait stability ratio variance were explained mostly by the second PLS component which mainly correlated with flortaucipir-PET uptake in the midbrain, basal ganglia and thalamus and with fractional anisotropy in the pontine crossing tract, medial lemniscus, corticospinal tract and superior and middle cerebellar peduncle. This component may point to a mechanism that regulates the speed and dynamic component of gait in PSP. The cerebellum plays an important role in maintaining balance (Tian et al. 2017) and its volume and flortaucipir-PET uptake, together with the vermis, emerged in the third PLS component as an important variable for explaining variance in cadence. The fact that, in this component, MRI volumes and flortaucipir SUVR had a concordant sign (i.e., both higher in patients with higher cadence) may point to heterogeneity within PSP as discussed above (Whitwell et al., 2020).

This study has some limitations. It is a cross-sectional study and therefore not suited to investigate causality. The number of participants is limited, particularly for FDG-PET, although comparable to previous studies (Zwergal et al. 2011, Zwergal et al. 2013, Palmisano et al. 2020), and did not allow us to correct for multiple comparisons. The limited number of patients did not allow for a detailed comparison across variants. However, the analyses performed in the sub-group of PSP-RS patients revealed some associations between imaging abnormalities and gait and balance impairments that were not present when all the phenotypes were analyzed together, suggesting that a comparison among variants is needed. Participants were diagnosed clinically and only one case underwent autopsy confirmation so far. Healthy controls were not recruited, hence discriminating PSP-specific relations from normal aging was not possible. *In vivo* tau pathology in PSP patients can be imaged with the PET ligand flortaucipir; however its use remains rather controversial because the tracer was optimized for the paired helical tau filaments typical of Alzheimer's disease and its off-target binding sites overlap with PSP regions of interest (Whitwell 2018, Leuzy et al. 2019).

5. Conclusions

We showed that gait and postural impairments in PSP are associated with imaging abnormalities on different sets of regions and tracts that belong to the PSP system of neurodegeneration and the supraspinal locomotor network. Our results suggest that gait and balance impairments might be driven by different mechanisms in PSP. Although larger longitudinal studies are needed, the data presented here may have implications in selecting biomarkers for clinical treatments trials that target movement abnormalities in PSP.

CRediT authorship contribution statement

Irene Sintini: Investigation, Supervision, Methodology, Formal analysis, Writing – original draft. **Kenton Kaufman:** Resources, Investigation, Writing – review & editing. **Hugo Botha:** Investigation, Writing – review & editing. **Peter R. Martin:** Methodology, Writing – review & editing. **Stacy R. Loushin:** Investigation, Data curation. **Matthew L. Senjem:** Software, Writing – review & editing. **Robert I. Reid:** Software, Writing – review & editing. **Christopher G. Schwarz:** Software, Writing – review & editing. **Clifford R. Jack Jr:** Resources, Writing – review & editing. **Val J. Lowe:** Investigation, Resources, Writing – review & editing. **Keith A. Josephs:** Funding acquisition, Investigation, Writing – review & editing. **Jennifer L. Whitwell:** Funding acquisition, Investigation, Writing – review & editing. **Farwa Ali:** Funding acquisition, Investigation, Writing – review & editing, Supervision, Conceptualization.

Acknowledgements

We would like to greatly thank AVID Radiopharmaceuticals, Inc., for their support in supplying the AV-1451 precursor, chemistry production advice and oversight, and FDA regulatory cross-filing permission and documentation needed for this work.

Funding

This study was funded by National Institutes of Health grants R01 NS89757, R01 DC12519 and internal neurology departmental grant part of UL1 TR002377 from the National Center for Advancing Translational Sciences (NCATS).

Competing interests

Dr. Val Lowe consults for Bayer Schering Pharma, Piramal Life Sciences, Life Molecular Imaging, Eisai Inc., AVID Radiopharmaceuticals, and Merck Research and receives research support from GE Healthcare, Siemens Molecular Imaging, AVID Radiopharmaceuticals and the NIH (NIA, NCI). Dr. Clifford R. Jack serves on a scientific advisory board for Eli Lilly & Company, as a speaker for Eisai and on an independent data safety monitoring board for Roche but he receives no personal compensation from any commercial entity; receives research support from the NIH, and the Alexander Family Alzheimer's Disease Research Professorship of the Mayo Clinic.

Appendix A. Supplementary data

Supplementary data to this article can be found online at https://doi.org/10.1016/j.nicl.2021.102850.

References

Ali, F., Loushin, S.R., Botha, H., Josephs, K.A., Whitwell, J.L., Kaufman, K., 2021. Laboratory based assessment of gait and balance impairment in patients with progressive supranuclear palsy. Journal of the Neurological Sciences 118054.

Amano, S., Skinner, J.W., Lee, H.K., Stegemoller, E.L., Hack, N., Akbar, U., Vaillancourt, D., McFarland, N.R., Hass, C.J., 2015. Discriminating features of gait performance in progressive supranuclear palsy. Parkinsonism & Related Disorders 21 (8), 888–893.

Amboni, M., Ricciardi, C., Picillo, M., De Santis, C., Ricciardelli, G., Abate, F., Tepedino, M.F., D'Addio, G., Cesarelli, G., Volpe, G., 2021. Gait analysis may distinguish progressive supranuclear palsy and Parkinson disease since the earliest stages. Scientific reports 11 (1), 1–9.

Bluett, B., I. Litvan, S. M. Cheng, J. Juncos, D. E. Riley, D. G. Standaert, S. G. Reich, D. A. Hall, B. Kluger, D. Shprecher, C. Marras, J. Jankovic and E. P. Study (2017). "Understanding falls in progressive supranuclear palsy." Parkinsonism & Related Disorders 35: 75-81.

Bohnen, N.I., Jahn, K., 2013. Imaging: What Can it Tell Us About Parkinsonian Gait? Movement Disorders 28 (11), 1492–1500.

Canu, E., Agosta, F., Baglio, F., Galantucci, S., Nemni, R., Filippi, M., 2011. Diffusion tensor magnetic resonance imaging tractography in progressive supranuclear palsy. Mov Disord 26 (9), 1752–1755.

Caruyer, E., Lenglet, C., Sapiro, G., Deriche, R., 2013. Design of multishell sampling schemes with uniform coverage in diffusion MRI. Magnetic resonance in medicine 69 (6), 1534–1540.

Chen, K.W., Reiman, E.M., Huan, Z.D., Caselli, R.J., Bandy, D., Ayutyanont, N., Alexander, G.E., 2009. Linking functional and structural brain images with multivariate network analyses: A novel application of the partial least square method. Neuroimage 47 (2), 602–610.

Chen, R., Lemon, R., 2004. Subthalamic nucleus and gait disturbance - Interactions between basal ganglia and brainstem and spinal pathways? Neurology 63 (7), 1150–1151.

Cope, T.E., Rittman, T., Borchert, R.J., Jones, P.S., Vatansever, D., Allinson, K., Passamonti, L., Rodriguez, P.V., Bevan-Jones, W.R., O'Brien, J.T., Rowe, J.B., 2018. Tau burden and the functional connectome in Alzheimer's disease and progressive supranuclear palsy. Brain 141, 550–567.

Cromwell, R.L., Newton, R.A., 2004. Relationship between balance and gait stability in healthy older adults. Journal of aging and physical activity 12 (1), 90–100.

De Vos, M., Prince, J., Buchanan, T., FitzGerald, J.J., Antoniades, C.A., 2020. Discriminating progressive supranuclear palsy from Parkinson's disease using wearable technology and machine learning. Gait & Posture 77, 257–263.

Dickson, D.W., Ahmed, Z., Algom, A.A., Tsuboi, Y., Josephs, K.A., 2010. Neuropathology of variants of progressive supranuclear palsy. Current Opinion in Neurology 23 (4), 394–400.

Duysens, J., Nonnekes, J., 2021. Parkinson's Kinesia Paradoxa Is Not a Paradox. Movement Disorders.

Egerton, T., Williams, D.R., Iansek, R., 2012. Comparison of gait in progressive supranuclear palsy, Parkinson's disease and healthy older adults. Bmc Neurology 12.

Ewert, S., Plettig, P., Li, N., Chakravarty, M.M., Collins, D.L., Herrington, T.M., Kühn, A. A., Horn, A., 2018. Toward defining deep brain stimulation targets in MNI space: a subcortical atlas based on multimodal MRI, histology and structural connectivity. Neuroimage 170, 271–282.

Heitmann, D.K., Gossman, M.R., Shaddeau, S.A., Jackson, J.R., 1989. Balance performance and step width in noninstitutionalized, elderly, female fallers and nonfallers. Physical therapy 69 (11), 923–931.

Hof, A.L., 2008. The 'extrapolated center of mass' concept suggests a simple control of balance in walking. Human Movement Science 27 (1), 112–125.

Hoglinger, G.U., Respondek, G., Stamelou, M., Kurz, C., Josephs, K.A., Lang, A.E., Mollenhauer, B., Muller, U., Nilsson, C., Whitwell, J.L., Arzberger, T., Englund, E., Gelpi, E., Giese, A., Irwin, D.J., Meissner, W.G., Pantelyat, A., Rajput, A., van Swieten, J.C., Troakes, C., Antonini, A., Bhatia, K.P., Bordelon, Y., Compta, Y., Corvol, J.C., Colosimo, C., Dickson, D.W., Dodel, R., Ferguson, L., Grossman, M., Kassubek, J., Krismer, F., Levin, J., Lorenzl, S., Morris, H.R., Nestor, P., Oertel, W.H., Poewe, W., Rabinovici, G., Rowe, J.B., Schellenberg, G.D., Seppi, K., van Eimeren, T., Wenning, G.K., Boxer, A.L., Golbe, L.I., Litvan, I., M. D. S.-E. PS,, 2017. Clinical Diagnosis of Progressive Supranuclear Palsy: The Movement Disorder Society Criteria. Movement Disorders 32 (6), 853–864.

Holland, N., Jones, P.S., Savulich, G., Wiggins, J.K., Hong, Y.T., Fryer, T.D., Manavaki, R., Sephton, S.M., Boros, I., Malpetti, M., Hezemans, F.H., Aigbirhio, F.I., Coles, J.P., O'Brien, J., Rowe, J.B., 2020. Synaptic Loss in Primary Tauopathies Revealed by [C-11]UCB-JPositron Emission Tomography. Movement Disorders 35 (10), 1834–1842.

Jahn, K., Deutschlander, A., Stephan, T., Kalla, R., Hufner, K., Wagner, J., Strupp, M., Brandt, T., 2008. Supraspinal locomotor control in quadrupeds and humans. Using Eye Movements as an Experimental Probe of Brain Function - a Symposium in Honor of Jean Buttner-Ennever 171, 353–362.

Josephs, K.A., Ishizawa, T., Tsuboi, Y., Cookson, N., Dickson, D.W., 2002. A clinicopathological study of vascular progressive supranuclear palsy - A multi-infarct disorder presenting as progressive supranuclear palsy. Archives of Neurology 59 (10), 1597–1601.

Josephs, K.A., Xia, R., Mandrekar, J., Gunter, J.L., Senjem, M.L., Jack Jr., C.R., Whitwell, J.L., 2013. Modeling trajectories of regional volume loss in progressive supranuclear palsy. Mov Disord 28 (8), 1117–1124.

Kammermeier, S., L. Dietrich, K. Maierbeck, A. Plate, S. Lorenzl, A. Singh, A. Ahmadi and K. Botzel (2018). "Postural Stabilization Differences in Idiopathic Parkinson's Disease and Progressive Supranuclear Palsy during Self-Triggered Fast Forward Weight Lifting." Frontiers in Neurology 8.

Kammermeier, S., Maierbeck, K., Dietrich, L., Plate, A., Lorenzl, S., Singh, A., Botzel, K., Maurer, C., 2018b. Qualitative postural control differences in Idiopathic Parkinson's Disease vs. Progressive Supranuclear Palsy with dynamic-on-static platform tilt. Clinical Neurophysiology 129 (6), 1137–1147.

Leuzy, A., Chiotis, K., Lemoine, L., Gillberg, P.G., Almkvist, O., Rodriguez-Vieitez, E., Nordberg, A., 2019. Tau PET imaging in neurodegenerative tauopathies-still a challenge. Molecular Psychiatry 24 (8), 1112–1134.

Liao, K., Wagner, J., Joshi, A., Estrovich, I., Walker, M.F., Strupp, M., Leigh, R.J., 2008. Why do patients with PSP fall? Evidence for abnormal otolith responses. Neurology 70 (10), 802–809.

Lindemann, U., Nicolai, S., Beische, D., Becker, C., Srulijes, K., Dietzel, E., Bauer, S., Berg, D., Maetzler, W., 2010. Clinical and Dual-Tasking Aspects In Frequent and Infrequent Fallers with Progressive Supranuclear Palsy. Movement Disorders 25 (8), 1040–1046.

Malpetti, M., Passamonti, L., Rittman, T., Jones, P.S., Rodriguez, P.V., Bevan-Jones, W. R., Hong, Y.T., Fryer, T.D., Aigbirhio, F.I., O'Brien, J.T., Rowe, J.B., 2020. Neuroinflammation and Tau Colocalize in vivo in Progressive Supranuclear Palsy. Annals of Neurology.

Morris, M.E., Iansek, R., Matyas, T.A., Summers, J.J., 1996. Stride length regulation in Parkinson's disease normalization strategies and underlying mechanisms. Brain 119, 551–568.

Nicastro, N., Rodriguez, P.V., Malpetti, M., Bevan-Jones, W.R., Simon Jones, P., Passamonti, L., Aigbirhio, F.I., O'Brien, J.T., Rowe, J.B., 2020. F-18-AV1451 PET imaging and multimodal MRI changes in progressive supranuclear palsy. Journal of Neurology 267 (2), 341–349.

Oishi, K., Faria, A., Jiang, H.Y., Li, X., Akhter, K., Zhang, J.Y., Hsu, J.T., Miller, M.I., van Zijl, P.C.M., Albert, M., Lyketsos, C.G., Woods, R., Toga, A.W., Pike, G.B., Rosa-Neto, P., Evans, A., Mazziotta, J., Mori, S., 2009. Atlas-based whole brain white matter analysis using large deformation diffeomorphic metric mapping: Application to normal elderly and Alzheimer's disease participants. Neuroimage 46 (2), 486–499.

Palmisano, C., Todisco, M., Marotta, G., Volkmann, J., Pacchetti, C., Frigo, C.A., Pezzoli, G., Isaias, I.U., 2020. Gait initiation in progressive supranuclear palsy: brain metabolic correlates. NeuroImage: Clinical 102408.

Passamonti, L., Rodriguez, P.V., Hong, Y.T., Allinson, K.S.J., Williamson, D., Borchert, R. J., Sami, S., Cope, T.E., Bevan-Jones, W.R., Jones, P.S., Arnold, R., Surendranathan, A., Mak, E., Su, L., Fryer, T.D., Aigbirhio, F.I., O'Brien, J.T., Rowe, J.B., 2017. F-18-AV-1451 positron emission tomography in Alzheimer's disease and progressive supranuclear palsy. Brain 140, 781–791.

Potter, M., Illert, M., Wenzelburger, R., Deuschl, G., Volkmann, J., 2004. The effect of subthalamic nucleus stimulation on autogenic inhibition in Parkinson disease. Neurology 63 (7), 1234–1239.

Price, S., Paviour, D., Scahill, R., Stevens, J., Rossor, M., Lees, A., Fox, N., 2004. Voxel-based morphometry detects patterns of atrophy that help differentiate progressive supranuclear palsy and Parkinson's disease. Neuroimage 23 (2), 663–669.

Raccagni, C., Gassner, H., Eschlboeck, S., Boesch, S., Krismer, F., Seppi, K., Poewe, W., Eskofier, B.M., Winkler, J., Wenning, G., Klucken, J., 2018. Sensor-based gait analysis in atypical parkinsonian disorders. Brain and Behavior 8 (6).

Rosenblatt, N.J., Grabiner, M.D., 2010. Measures of frontal plane stability during treadmill and overground walking. Gait & Posture 31 (3), 380–384.

Schonhaut, D.R., McMillan, C.T., Spina, S., Dickerson, B.C., Siderowf, A., Devous, M.D., Tsai, R., Winer, J., Russell, D.S., Litvan, I., Roberson, E.D., Seeley, W.W., Grinberg, L. T., Kramer, J.H., Miller, B.L., Pressman, P., Nasrallah, I., Baker, S.L., Gomperts, S.N., Johnson, K.A., Grossman, M., Jagust, W.J., Boxer, A.L., Rabinovici, G.D., 2017. F-18-flortaucipir tau positron emission tomography distinguishes established progressive supranuclear palsy from controls and Parkinson disease: A multicenter study. Annals of Neurology 82 (4), 622–634.

Schwarz, C.G., Reid, R.I., Gunter, J.L., Senjem, M.L., Przybelski, S.A., Zuk, S.M., Whitwell, J.L., Vemuri, P., Josephs, K.A., Kantarci, K., Thompson, P.M., Petersen, R. C., Jack, C.R., A. s. D. N. Initi,, 2014. Improved DTI registration allows voxel-based analysis that outperforms Tract-Based Spatial Statistics. Neuroimage 94, 65–78.

Sintini, I., Schwarz, C.G., Senjem, M.L., Reid, R.I., Botha, H., Ali, F., Ahlskog, J.E., Jack, C.R., Lowe, V.J., Josephs, K.A., Whitwell, J.L., 2019. Multimodal neuroimaging relationships in progressive supranuclear palsy. Parkinsonism & Related Disorders 66, 56–61.

Smith, R., Schain, M., Nilsson, C., Strandberg, O., Olsson, T., Hagerstrom, D., Jogi, J., Borroni, E., Scholl, M., Honer, M., Hansson, O., 2017. Increased Basal Ganglia Binding of F-18-AV-1451 in Patients With Progressive Supranuclear Palsy. Movement Disorders 32 (1), 108–114.

Sutherland, D., Olshen, R., Biden, E., 1988. The development of mature walking. Cambridge University Press.

Tian, Q., Chastan, N., Bair, W.N., Resnick, S.M., Ferrucci, L., Studenski, S.A., 2017. The brain map of gait variability in aging, cognitive impairment and dementia A systematic review. Neuroscience and Biobehavioral Reviews 74, 149–162.

Tian, Q., Ferrucci, L., Resnick, S.M., Simonsick, E.M., Shardell, M.D., Landman, B.A., Venkatraman, V.K., Gonzalez, C.E., Studenski, S.A., 2016a. The effect of age and microstructural white matter integrity on lap time variation and fast-paced walking speed. Brain Imaging and Behavior 10 (3), 697–706.

Tian, Q., Resnick, S.M., Landman, B.A., Huo, Y.K., Venkatraman, V.K., Gonzalez, C.E., Simonsick, E.M., Shardell, M.D., Ferrucci, L., Studenski, S.A., 2016b. Lower gray matter integrity is associated with greater lap time variation in high-functioning older adults. Experimental Gerontology 77, 46–51.

Verlinden, V.J.A., de Groot, M., Cremers, L.G.M., van der Geest, J.N., Hofman, A., Niessen, W.J., van der Lugt, A., Vernooij, M.W., Ikram, M.A., 2016. Tract-specific white matter microstructure and gait in humans. Neurobiology of Aging 43, 164–173.

Whitwell, J.L., 2018. Tau Imaging in Parkinsonism: What Have We Learned So Far? Movement Disorders Clinical Practice 5 (2), 118–130.

Whitwell, J.L., Avula, R., Master, A., Vemuri, P., Senjem, M.L., Jones, D.T., Jack, C.R., Josephs, K.A., 2011a. Disrupted thalamocortical connectivity in PSP: a resting state fMRI, DTI, and VBM study. Parkinsonism Relat Disord 17 (8), 599–605.

Whitwell, J.L., Lowe, V.J., Tosakulwong, N., Weigand, S.D., Senjem, M.L., Schwarz, C.G., Spychalla, A.J., Petersen, R.C., Jack Jr., C.R., Josephs, K.A., 2017. [18 F]AV-1451 tau positron emission tomography in progressive supranuclear palsy. Mov Disord 32 (1), 124–133.

Whitwell, J.L., Master, A.V., Avula, R., Kantarci, K., Eggers, S.D., Edmonson, H.A., Jack Jr., C.R., Josephs, K.A., 2011b. Clinical correlates of white matter tract degeneration in progressive supranuclear palsy. Arch Neurol 68 (6), 753–760.

Whitwell, J. L., N. Tosakulwong, H. Botha, F. Ali, H. M. Clark, J. R. Duffy, R. L. Utianski, C. A. Stevens, S. D. Weigand, C. G. Schwarz, M. L. Senjem, C. R. Jack, V. J. Lowe, J. E. Ahlskog, D. W. Dickson and K. A. Josephs (2020). "Brain volume and flortaucipir analysis of progressive supranuclear palsy clinical variants." Neuroimage-Clinical 25.

Whitwell, J.L., Tosakulwong, N., Clark, H.M., Ali, F., Botha, H., Weigand, S.D., Sintini, I., Machulda, M.M., Schwarz, C.G., Reid, R.I., Jack, C.R., Ahlskog, J.E., Josephs, K.A., 2021. Diffusion tensor imaging analysis in three progressive supranuclear palsy variants. Journal of Neurology.

Whitwell, J.L., Tosakulwong, N., Schwarz, C.G., Botha, H., Senjem, M.L., Spychalla, A.J., Ahlskog, J.E., Knopman, D.S., Petersen, R.C., Jack, C.R., Lowe, V.J., Josephs, K.A., 2019. MRI Outperforms [18F]AV-1451 PET as a Longitudinal Biomarker in Progressive Supranuclear Palsy. Movement Disorders 34 (1), 105–113.

Zwergal, A., la Fougere, C., Lorenzl, S., Rominger, A., Xiong, G., Deutschenbaur, L., Linn, J., Krafczyk, S., Dieterich, M., Brandt, T., Strupp, M., Bartenstein, P., Jahn, K., 2011. Postural imbalance and falls in PSP correlate with functional pathology of the thalamus. Neurology 77 (2), 101–109.

Zwergal, A., la Fougere, C., Lorenzl, S., Rominger, A., Xiong, G.M., Deutschenbaur, L., Schoberl, F., Linn, J., Dieterich, M., Brandt, T., Strupp, M., Bartenstein, P., Jahn, K., 2013. Functional disturbance of the locomotor network in progressive supranuclear palsy. Neurology 80 (7), 634–641.